

Original citation:

Pages, Benjamin J., Sakoff, Jennette, Gilbert, Jayne, Rodger, Alison, Chmel, Nikola P., Jones, Nykola C., Kelly, Sharon M., Ang, Dale L. and Aldrich-Wright, Janice R.. (2016) Multifaceted studies of the DNA interactions and in vitro cytotoxicity of anticancer polyaromatic platinum(II) complexes. *Chemistry - A European Journal*, 22 (26). pp. 8943-8954.

Permanent WRAP URL:

<http://wrap.warwick.ac.uk/80972>

Copyright and reuse:

The Warwick Research Archive Portal (WRAP) makes this work by researchers of the University of Warwick available open access under the following conditions. Copyright © and all moral rights to the version of the paper presented here belong to the individual author(s) and/or other copyright owners. To the extent reasonable and practicable the material made available in WRAP has been checked for eligibility before being made available.

Copies of full items can be used for personal research or study, educational, or not-for profit purposes without prior permission or charge. Provided that the authors, title and full bibliographic details are credited, a hyperlink and/or URL is given for the original metadata page and the content is not changed in any way.

Publisher's statement:

"This is the peer reviewed version of the following article: Pages, Benjamin J., Sakoff, Jennette, Gilbert, Jayne, Rodger, Alison, Chmel, Nikola P., Jones, Nykola C., Kelly, Sharon M., Ang, Dale L. and Aldrich-Wright, Janice R.. (2016) Multifaceted studies of the DNA interactions and in vitro cytotoxicity of anticancer polyaromatic platinum(II) complexes. *Chemistry - A European Journal*, 22 (26). pp. 8943-8954. which has been published in final form at <http://dx.doi.org/10.1002/chem.201601221> This article may be used for non-commercial purposes in accordance with [Wiley Terms and Conditions for Self-Archiving](#)."

A note on versions:

The version presented here may differ from the published version or, version of record, if you wish to cite this item you are advised to consult the publisher's version. Please see the 'permanent WRAP URL' above for details on accessing the published version and note that access may require a subscription.

For more information, please contact the WRAP Team at: wrap@warwick.ac.uk

Multifaceted studies of the DNA interactions and *in vitro* cytotoxicity of anticancer polyaromatic platinum(II) complexes

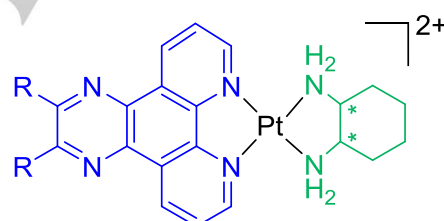
Benjamin J. Pages,^[a] Jennette Sakoff,^[b] Jayne Gilbert,^[b] Alison Rodger,^[c] Nikola P. Chmel,^[c] Nykola C. Jones,^[d] Sharon M. Kelly,^[e] Dale L. Ang,^[a] Janice R. Aldrich-Wright.^{*[a]}

Abstract: This paper reports a detailed biophysical analysis of the DNA binding and cytotoxicity of six platinum complexes (PCs). They are of the type $[\text{Pt}(\text{P}_L)(\text{SS-dach})\text{Cl}_2]$, where P_L is a polyaromatic ligand and SS-dach is 1*S*,2*S*-diaminocyclohexane. The DNA binding of these complexes was investigated using six techniques including ultraviolet and fluorescence spectroscopy, linear dichroism, synchrotron radiation circular dichroism, isothermal titration calorimetry and mass spectrometry. This portfolio of techniques has not been extensively used to study the interactions of such complexes previously; each assay provided unique insight. The *in vitro* cytotoxicity of these compounds was studied in ten cell lines and compared to the effects of their *R,R* enantiomers; activity was very high in Du145 and SJ-G2 cells, with some sub-micromolar IC_{50} values. In terms of both DNA affinity and cytotoxicity, complexes of 5,6-dimethyl-1,10-phenanthroline and 2,2'-bipyridine exhibited the greatest and least activity, respectively, suggesting that there is some correlation between DNA binding and cytotoxicity.

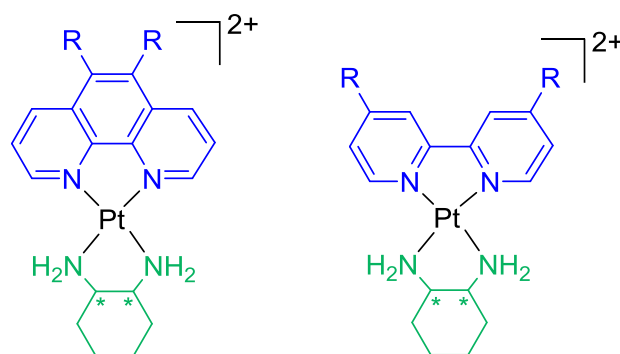
Introduction

A long-standing aspiration of medicinal inorganic chemists has been the development of chemotherapeutic agents that can effectively combat cancerous cells, yet overcome the resistance and toxicity that plague current clinically used platinum agents.^[1] Platinum complexes (PCs) with mechanisms of action quite different from current agents have been explored as alternatives, and have demonstrated *in vitro* cytotoxicity up to 100 times

greater than cisplatin in several cell lines.^[2] In particular, our group has focused on the development of PCs that consist of a polyaromatic ligand (P_L) and a cyclic amine ancillary ligand (A_L) in the form $[\text{Pt}(\text{P}_L)(\text{A}_L)]^{2+}$.^[3] These complexes interact non-covalently with DNA, often *via* intercalation, rather than by forming permanent adducts. They also induce cell death by a different mechanism than cisplatin,^[2a, 4] and are potently cytotoxic against a variety of cell lines, including some that are cisplatin-resistant.^[5] Our previous studies have been inconclusive as to whether there is a correlation between DNA affinity and cytotoxicity; however, these studies have often used only one or two spectroscopic techniques to study PC-DNA interactions.^[6] Moreover, DNA binding affinity is known to vary depending on the method of measurement and the conditions used, and so separately conducted studies can often provide inconsistent results.^[7] In this study, we have utilised several biophysical assays to study the interactions of six PCs with DNA (Figure 1).



R = H, S,S: Complex 1, **DPQSS**
 R = H, R,R: Complex 1', **DPQRR**
 R = CH₃, S,S: Complex 2, **23MEDSS**
 R = CH₃, S,S: Complex 2', **23MEDRR**



R = H, S,S: Complex 3, **PHENSS**
 R = H, R,R: Complex 3', **PHENRR**
 R = CH₃, S,S: Complex 4, **56MESS**
 R = CH₃, S,S: Complex 4', **56MERR**
 R = H, S,S: Complex 5, **BPYSS**
 R = H, R,R: Complex 5', **BPYRR**
 R = CH₃, S,S: Complex 6, **44MEBSS**
 R = CH₃, S,S: Complex 6', **44MEBRR**

- [a] Mr Benjamin J. Pages, Mr Dale L. Ang, Prof Janice R. Aldrich-Wright
 Nanoscale Organisation and Dynamics Group
 Western Sydney University
 Campbelltown, NSW 2560, Australia
 E-mail: j.aldrich-wright@westernsydney.edu.au
- [b] Dr Jennette Sakoff, Dr Jayne Gilbert
 Calvary Mater Newcastle
 Waratah, NSW 2298, Australia
- [c] Prof Alison Rodger, Dr Nikola P. Chmel
 Department of Chemistry
 University of Warwick
 Coventry, West Midlands CV47AL, United Kingdom
- [d] Dr Nykola C. Jones
 ISA, Department of Physics and Astronomy
 Aarhus University
 Aarhus 8000, Denmark
- [e] Dr Sharon Kelly
 Institute of Molecular, Cell and Systems Biology, College of
 Medical, Veterinary and Life Sciences
 University of Glasgow
 Glasgow G128QQ, United Kingdom

Figure 1. The structures of complexes 1–6 and 1'–6'; each A_L is highlighted in green and each P_L in blue. Chloride counter ions have been omitted for clarity. * indicates a stereocentre, either S or R.

The experimental conditions were kept consistent, where possible, for each assay to facilitate comparison of the binding data elucidated from the individual techniques. This allowed for definitive trends in DNA binding affinity to be determined for the six PCs. The complexes studied here incorporated 1*S*,2*S*-diaminocyclohexane (SS-dach) as an A_L and one of dipyrido[3,2-*d*:2',3'-*f*]quinoxaline (dpq), 2,3-dimethyl-dpq (23Me₂dpq), 1,10-phenanthroline (phen), 5,6-dimethyl-phen (56Me₂phen), 2,2'-bipyridine (bpy) and 4,4'-dimethyl-bpy (44Me₂bpy) as an P_L . The use of a variety of P_L s allowed for a comparison between the DNA affinity and aromatic surface area of these complexes; it is known that structural variations can result in different DNA binding behaviour for metal complexes.^[8] Methylated variants of each P_L were included due to the proven cytotoxic and DNA binding influences of methyl substituents in our complexes,^[3, 5b] and SS-dach was chosen as the A_L as complexes of this ligand are the most active overall.^[5b] The interactions of complexes **1–6** with calf-thymus DNA (CT-DNA) and some oligonucleotides were analysed using several methods. Firstly, linear dichroism (LD), ultraviolet spectroscopy (UV) and isothermal titration calorimetry (ITC) were utilised in tandem to gain an overall picture of DNA binding mode and affinity. Secondly, fluorescent intercalator displacement assays (FIDs) and synchrotron radiation circular dichroism (SRCD) experiments were undertaken to determine the effect of DNA affinity on the ability of each complex to displace competitive binders and stabilise the DNA strand, respectively. Thirdly, electrospray ionisation mass spectrometry (ESIMS) was used to determine if **1–6** preferentially bind to any base-pairs. Finally, the cytotoxicity of these compounds was determined in ten human cell lines. The activity of **1–6** was compared to their enantiomers **1'–6'** and to the DNA binding results to determine any correlations between chemical structure, DNA affinity and cytotoxicity.

Results and Discussion

Linear dichroism

The LD spectrum of CT-DNA is characterised by a large negative band at ~260 nm. Upon the addition of each PC in this study, the band at 260 nm increased in intensity, which suggests a lengthening or stiffening of the DNA strand. Additionally, negative LD signals appeared at the absorbance wavelengths of each PC, which suggests that their aromatic components have aligned perpendicular to the DNA strand. The PC signals were flattened, broadened and red-shifted relative to their absorbance bands (Figure 2). These phenomena together indicate that each PC is binding *via* intercalation to DNA. While the alignment of complex **6** is obvious from the LD signal at 321 nm, this complex also absorbs at 243 and 206 nm; the same region as CT-DNA. The increase of the 260 nm LD peak upon addition of **6** could therefore be due to PC alignment only and not a result of DNA lengthening. To elucidate the cause of the signal change, the UV spectra of **6** and CT-DNA were compared to the induced LD signal of DNA+**6** (Figure 3). In the induced LD spectrum, the peak at 247 nm has a higher relative intensity than the other

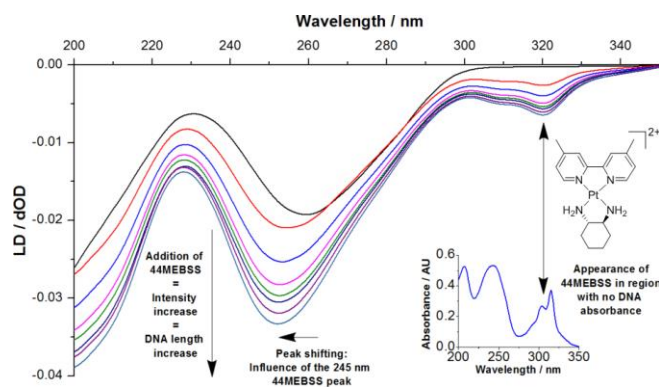


Figure 2. LD spectra of CT-DNA (150 μ M) with increasing concentration of complex **6** (selected concentrations from 40 – 200 μ M). Inset: The UV spectrum of **6**. See Figure S1.6 for spectra of the full concentration range.

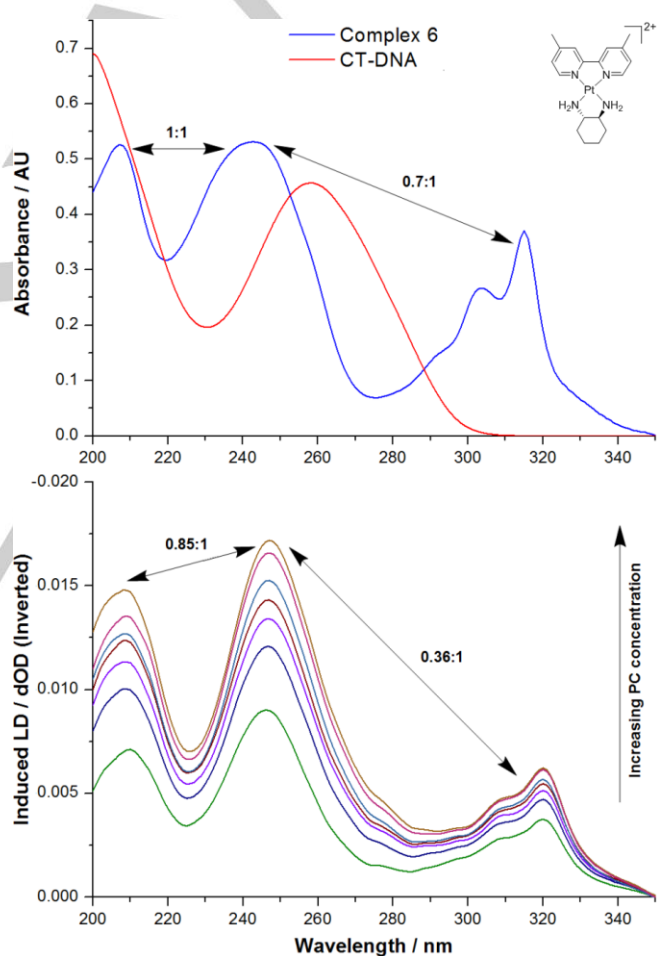


Figure 3. Top: The UV spectrum of CT-DNA (red line, 35 μ M) and complex **6** (blue line, 21 μ M), showing ratios to the peak at 243 nm for the former. Bottom: The inverted induced LD spectra of CT-DNA (150 μ M) bound with 44MEBSS (selected concentrations from 50–200 μ M), showing ratios to the peak at 247 nm.

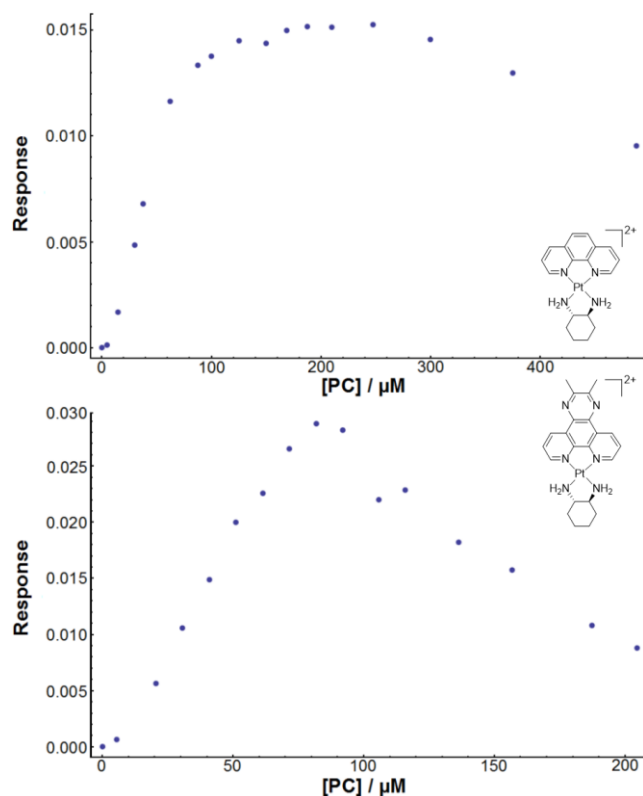


Figure 4. Plots of PC concentration against LD response of CT-DNA (150 μM) bound with increasing concentrations of complex **3** at 278 nm (4–488 μM , top) and **2** at 260 nm (5–205 μM , bottom).

two; this indicates that both the alignment of **6** and the lengthening of the DNA strand are both occurring, confirming that intercalation is the binding mode. Similar absorbance contributions were observed for each of complexes **1–5** as they all absorb in the same region as CT-DNA. For all PCs studied, there are two regions of the titration curve at which the signal in the CT-DNA region did not consistently increase with increasing PC concentration, despite the spectral evidence for DNA lengthening and/or stiffening. The first of these was a decrease or only very small increase of DNA signal intensity at 260 nm for PC concentrations between 5 and 30 μM . This may be indicative of a partial intercalation mode that hinges the DNA and bends it rather than full intercalation. The second point at which the LD signal did not increase was at high PC concentrations (85–100 μM); at this point a plateau was reached for complexes **1, 3, 5** and **6** before the signal began to decrease at ~ 250 μM (Figure 4). This suggests that the DNA reached saturation by intercalation before another binding mode occurred, which then caused the strand to lose its aspect ratio. An electrostatic groove binding mode of some kind is likely as the second **one**. The plateau allowed for a binding constant to be determined for the first or putative intercalative binding. For complexes **2** and **4**, the signal loss began to occur before any plateau was reached (at approx. 80 and 100 μM , respectively), implying that the second binding mode occurred earlier for these complexes than for the others (Figure 4). This made binding constant calculation

impossible, and suggests that the difference in binding strength of the two modes is less for these complexes **than it is for the others**. K_{LD} was determined for **1, 3, 5** and **6** using binding curves from either one or two peaks in the induced spectrum; the average data is presented in Table 1 (see Table S1.2 for individual wavelength data). The points of the binding curve below 40 μM had to be removed in order to obtain a fit; this was due to the aforementioned DNA bending at these concentrations. The peak at ~ 320 nm for complexes **5** and **6** were not a result of DNA absorbance and so could be fitted with all points below 40 μM . Each complex was found to bind to DNA with high potency. The intercalative binding strength of these PCs is attributed to stabilised π - π stacking as well as the longer range charge-charge interactions of the platinum cations.^[9] Complex **1** has the largest aromatic surface area and a binding constant of $\sim 10^6$ M^{-1} . The other complexes had similar K_{LD} values of 10^5 M^{-1} . n (number of base-pairs per PC) values were typically around 2–3, indicating that each PC could intercalate between every second or third base pair in a sequence. Despite the lack of some binding data for complexes **2** and **4**, LD has provided useful information regarding the binding activity of the PCs in this study.

UV binding assays

UV spectroscopy is a common method used to determine binding mode and affinity of metal complex-DNA interactions.^[10] The addition of DNA to each of complexes **1–6** resulted in hypochromism, with a varying shift in wavelength between the PCs (Figure 5). The spectra of **3–6** were red-shifted with the effect being more subtle for **5** and **6**, while the spectra of **1** and **2** experienced a blue-shift upon the addition of CT-DNA. Typically these shifting patterns can provide information regarding the DNA binding mode;^[10a] however, each of **1–6** absorb in the same region as DNA and so no definitive binding mode statements could be made from this data. Unlike the LD experiments, binding **constant** data was obtainable for all complexes in this instance, with no removal of binding curve points required (Figure 5). The possible secondary groove binding mode that limited the binding curves in LD had no effect here, and so the K_{UV} values are likely reflective of an overall binding affinity rather than just an intercalation-related one. Due to the differences in the UV spectra of each complex, different wavelengths were chosen for each K_{UV} determination. Where applicable, up to three wavelengths were chosen to facilitate a comparison between each value obtained; only minor differences were observed, and so the values in Table 1 are averages (see Table S2.2 for individual wavelength data). The K_{UV} did not vary considerably with aromatic surface area, with most binding constants close to 10^5 M^{-1} . The only exception is complex **4**, which demonstrated higher DNA affinity with a K_{UV} of $\sim 10^6$ M^{-1} . This suggests that the 56Me₂phen ligand, despite possessing a smaller aromatic surface than dpq or 23Me₂dpq, is the optimum DNA-binding P_L. Despite the lack of binding mode information relative to LD, UV spectroscopy has provided binding information for all concentration ranges without being restricted to one binding event. This in turn has allowed for binding data to be obtained for complexes **2** and **4** whereas LD could not do so.

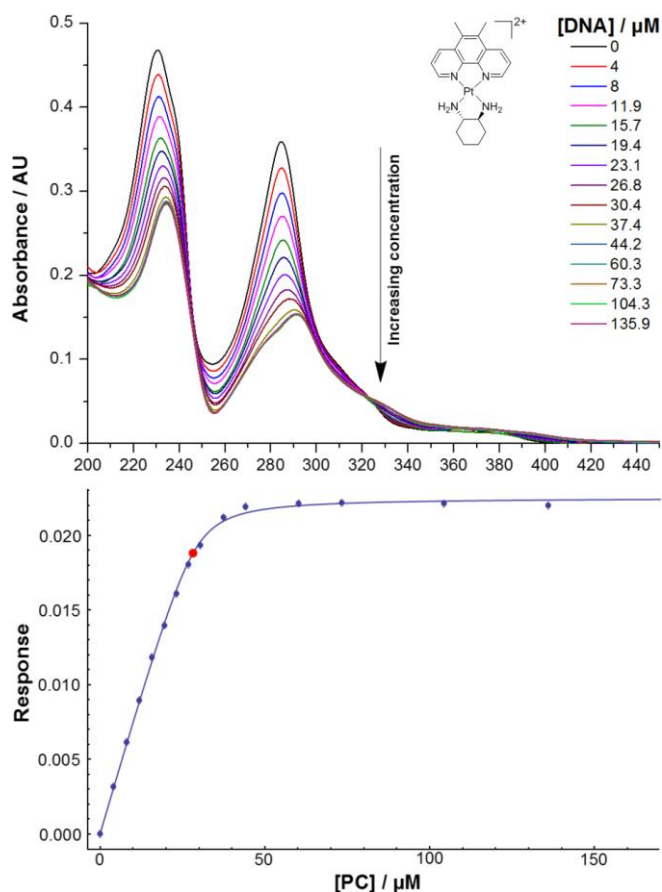


Figure 5. UV data for complex **4**: spectra at various DNA concentrations (top), and fitted binding curve produced by the Mathematica script (bottom). The red dot indicates that the fit was successful.^[11]

Isothermal titration calorimetry

ITC was employed here as it provides an overall picture of PC-DNA binding interaction from a calorimetric perspective.^[12] The titration of each of complexes **1–6** was exothermic in nature, with negative $\mu\text{cal sec}^{-1}$ peaks present that represent DNA binding events, followed by smaller peaks from the heat of dilution once the binding sites were exhausted (Figure 6). Many titrations resulted in the appearance of two peaks rather than one, or at least evidence of two merged peaks to give the appearance of one. This suggests that binding may be biphasic in nature; the second peak may result from the ejection of solvent or sodium from the DNA sites, or from a DNA conformational adjustment post-binding, or both. The calculated thermodynamic parameters for each of **1–6** were similar. The binding of each complex with CT-DNA was an exothermic event, with ΔH values ranging from -1000 to $-6000 \text{ cal mol}^{-1}$ and ΔS values between 8 and $20 \text{ cal mol}^{-1} \text{ deg}^{-1}$ (Table 3). The positive ΔS is likely due to the solvation entropy that results from the ejection of solvent molecules from the grooves of DNA during PC-DNA binding.^[13] The calculated ΔG values ranged between -7500 and $-8500 \text{ cal mol}^{-1}$. Complexes **3** and **5** exhibited the lowest binding constants of $\sim 2 \times 10^5 \text{ M}^{-1}$, while the values for **1, 2**

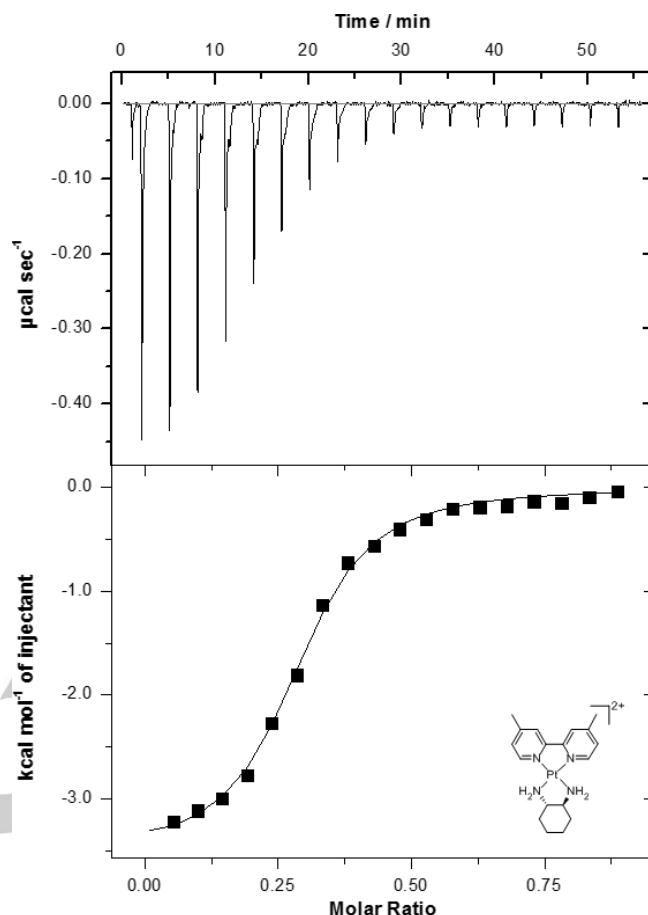


Figure 6. ITC trace and binding curve of the titration of complex **6** ($650 \mu\text{M}$) into CT-DNA ($164 \mu\text{M}$). Fits were obtained using a one-site binding model.

and **6** were $\sim 3 \times 10^5 \text{ M}^{-1}$. The only complex that appeared to bind with a distinctly higher affinity was complex **4** with a K_{ITC} of $(5.7 \pm 0.5) \times 10^5 \text{ M}^{-1}$. This again suggests that **56Me₂phen** is of an optimal size for DNA binding affinity. The number of PCs bound per base pair was between 0.25 and 0.3 ; converting that to n values reveals that approximately $3\text{--}4$ binding sites are present per PC.

Binding constant data comparison

Overall, LD, UV and ITC have each provided valuable insight into the binding of complexes **1–6** to CT-DNA. LD has provided definitive evidence for an intercalative binding mode, however it could only provide binding constants for this interaction for four of the studied PCs. Evidence for a second electrostatic groove binding mode was also found in the LD spectra. UV spectroscopy provided binding data for all of **1–6** that resulted from the overall binding interaction; however no binding mode information could be obtained. ITC produced similar binding constants to the UV data, as well as additional thermodynamic information that could not be gained from the spectroscopic techniques. Each technique measures different aspects of PC-DNA binding; LD quantified the intercalation event only, whereas

Table 1. Summary of binding constant data obtained from LD (150 μM CT-DNA + 40-200 μM PC), UV (15 μM PC + 7-200 μM CT-DNA) and ITC (titration of 600-750 μM PC into 165 μM CT-DNA) experiments. Standard deviation values are included (1 sig. fig.).

No.	LD Data		UV Data		ITC Data		ITC Data		
	$10^{-5} K_{\text{LD}} / \text{M}^{-1}$	n	$10^{-5} K_{\text{UV}} / \text{M}^{-1}$	n	$10^{-5} K / \text{M}^{-1}$	n	$\Delta H / \text{kcal mol}^{-1}$	$T\Delta S / \text{kcal mol}^{-1}$	$\Delta G / \text{kcal mol}^{-1}$
1	15.2 ± 0.4	2.41 ± 0.06	3.6 ± 0.2	3.13 ± 0.09	3.2 ± 0.3	3.98 ± 0.06	-4.4 ± 0.1	3.4 ± 0.1	-7.8 ± 0.3
2 ^[a]	-	-	4.7 ± 0.1	2.52 ± 0.01	2.8 ± 0.4	3.51 ± 0.08	-4.5 ± 0.1	3.2 ± 0.3	-7.7 ± 0.8
3	2.8 ± 0.4	2.2 ± 0.2	2.9 ± 0.4	3.5 ± 0.3	2.0 ± 0.3	3.7 ± 0.1	-3.7 ± 0.1	3.9 ± 0.4	-7.5 ± 0.7
4 ^[a]	-	-	13 ± 1	2.32 ± 0.02	5.7 ± 0.5	3.00 ± 0.02	-5.6 ± 0.1	2.6 ± 0.2	-8.2 ± 0.6
5 ^[b]	2.1 ± 0.3	3.1 ± 0.3	0.79 ± 0.06	4.4 ± 0.2	2.2 ± 0.4	3.4 ± 0.1	-1.3 ± 0.1	6.2 ± 0.2	-7.6 ± 0.4
6 ^[b]	3.0 ± 0.5	2.1 ± 0.2	5.2 ± 0.6	2.87 ± 0.04	3.2 ± 0.4	3.57 ± 0.06	-3.6 ± 0.1	4.2 ± 0.1	-7.8 ± 0.2

[a] LD values could not be determined due to a decrease in LD signal at high concentrations

[b] LD values also reflect data in which binding data points below 40 μM could be fitted

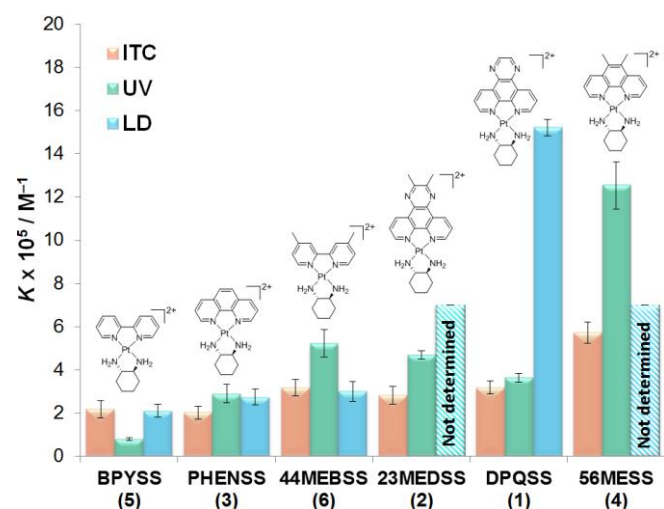


Figure 7. Comparison of the binding constants of complexes 1-6 with CT-DNA, as determined by ITC (red), UV (green) and LD (blue). Where applicable, K values over multiple wavelengths have been averaged for LD and UV data.

UV and ITC provided data that was representative of the overall interaction from a spectroscopic and calorimetric perspective, respectively. Therefore it is not surprising that there were some differences in the calculated binding data across each technique (Table 1). More importantly, trends in DNA affinity for complexes 1-6 are generally the same across all studies: $4 > 2 = 1 \geq 6 = 3 \geq 5$ (Figure 7). It is clear that these techniques are complementary and can each provide important information regarding PC-DNA binding.

Fluorescent intercalator displacement (FID) assays

The ability to displace competing ligands from a target is a crucial factor in the efficacy of a drug. To study the ability of complexes 1-6 to competitively displace other binders from CT-DNA, fluorescent intercalator displacement assays (FIDs) were utilised. Ethidium bromide (EtBr) was used here as it is fluorescent only when bound with DNA.^[14] The peak of emission for DNA-bound EtBr is at ~ 601 nm; upon the addition of each PC, the emission intensity decreased, indicating that some EtBr had been displaced from the DNA strand (Figure 8). EtBr is postulated to occupy several binding sites of DNA with an

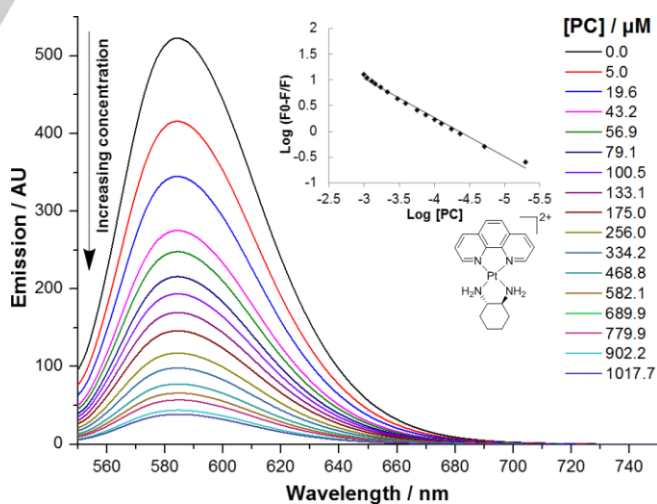


Figure 8. Emission spectra of DNA (150 μM) bound with EtBr (75 μM) with increasing concentration of complex 3. Inset: the double-logarithm plot used to determine K_f .

overall K_F of $\sim 10^5$ M.^[15] Therefore, the determination of an accurate displacement binding constant is a difficult task as there are several possible sites occupied by EtBr that can be displaced by groove binders and intercalators alike. The binding curves obtained in this study did not reach a plateau, even at [DNA]: [PC] ratios as low as 0.15; this indicates that some ethidium molecules could not be displaced from particular binding sites. The curves could subsequently not be fitted using the same processing method as the LD and UV data, and so a simplified processing method of a previous study of ours was used (see Experimental for details).^[6b] The results are summarised in Figure 9 and Table 2.

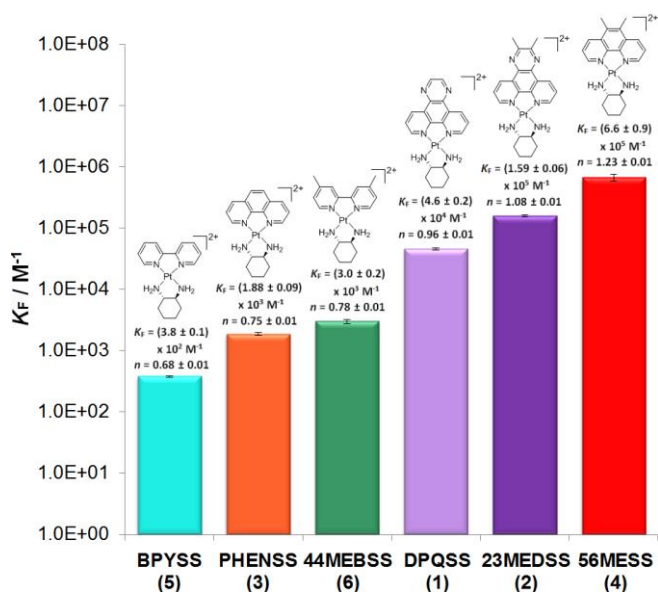


Figure 9. Comparison of the K_F and n determined for each PC, expressed on a logarithmic scale. Standard deviations (first significant figure) are included.

Table 2. Fluorescence constants calculated for complexes 1–6, expressed with standard deviation (1 sig. fig.).

No.	$10^{-5} K_q / M^{-1} s^{-1}$	$10^{-5} K_F / M^{-1}$	n
1	2.81 ± 0.03	0.46 ± 0.02	0.96 ± 0.01
2	3.41 ± 0.02	1.59 ± 0.06	1.08 ± 0.01
3	0.539 ± 0.009	0.019 ± 0.001	0.75 ± 0.01
4	3.7 ± 0.1	6.6 ± 0.9	1.23 ± 0.01
5	0.174 ± 0.004	0.0038 ± 0.0001	0.68 ± 0.01
6	0.67 ± 0.01	0.030 ± 0.002	0.78 ± 0.01

Each of the PCs studied was capable of displacing EtBr from the CT-DNA strand, with K_F values between 10^2 and 10^7 M⁻¹. The simplified processing method means that K_F is only an indication of the ability of the complex to displace ethidium, and is not

quantitatively representative of the binding affinity. Similarly, the calculated n values are representative of the amount of EtBr each complex can replace, rather than the number of DNA binding sites, and so it is logical that n values increased with increasing K_F . Each PC demonstrated K_q values above $\sim 2 \times 10^{10}$ M⁻¹ s⁻¹, indicating that EtBr displacement occurred prior to the measurement of emission.^[16] The trends between complexes 1–6 were still relatively consistent with the other data collected in this study; 4 and 5 demonstrated the highest and lowest affinity for CT-DNA, respectively. Greater differences were distinguishable between the rest of the complexes, suggesting that even the smallest differences in DNA affinity can result in large differences in competitive displacement ability that may be physiologically relevant.

Synchrotron radiation circular dichroism

SRCD has been used here to determine the effect of the binding of complexes 1–6 on the stability of CT-DNA. This was achieved through the determination of T_M , the temperature inflexion point at which the CD signal is lost due to a loss of secondary structure.^[17] The addition of each PC to CT-DNA resulted in dramatic changes in the SRCD spectrum, presumably due to conformational changes that occurred upon binding. The wavelength maxima and minima chosen for melting analysis differed for each of 1–6 as each complex influenced the CT-DNA spectrum in different ways. For each DNA-PC combination, CD signal decreased with increasing temperature (Figure 10), with melting occurring at different points for each PC. For each melting curve, the T_M did not vary significantly between the wavelengths chosen. The binding of all complexes to DNA resulted in a higher T_M than the average DNA value of 55 ± 1 °C (Figure 11). An increase in T_M is expected for intercalative binders. It is important to note that the binding curves for

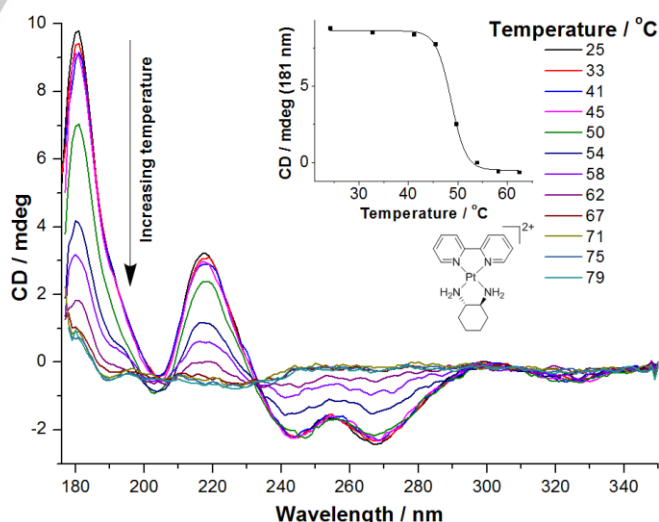


Figure 10. SRCD spectra of CT-DNA (1 mM) bound with complex 5 (0.5 mM) at various temperatures. Inset: the melting curve used to generate the T_M value (points past 62 °C have been omitted for clarity).

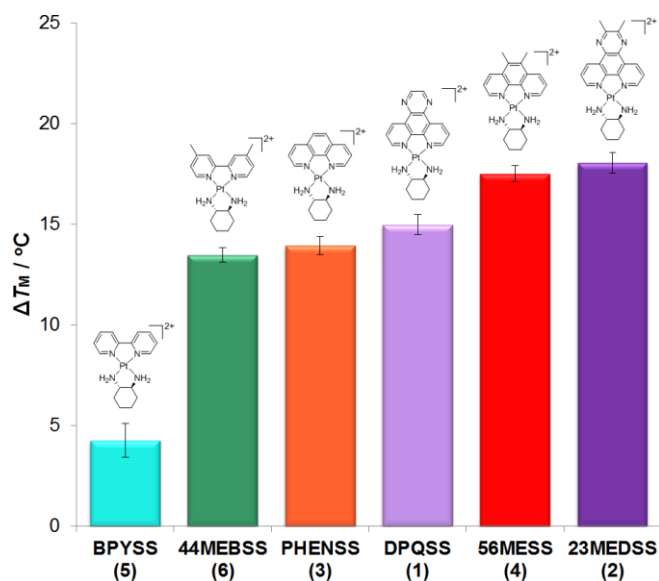


Figure 11. Comparison of the SRCD ΔT_M determined for CT-DNA bound with complexes 1–6. Standard deviations (error bars) are included.

complexes 2 and 4 (Section S5) barely reached completion as the hardware could not raise the temperature above ~ 79 °C; however, ΔT_M values were consistent between replicates. The trends in T_M for each complex were almost the same as the trends of the fluorescence study; the order of DNA stabilisation was $2 \cong 4 > 1 > 3 \cong 6 > 5$. Similarly to the FID assays, it appears that even minor differences in the DNA affinity of these PCs has led to large differences in their ability to stabilise helical DNA against melting.

Mass Spectrometry Binding Studies

Mass spectrometry is often used to probe ligand-biomolecule interactions at different stoichiometry.^[18] The mass spectra of each of the double complementary strands 5'-GCGCATGCGCATGCGC-3' ("GC Strand" or GCS) and 5'-GCATATGATATCATATGC-3' ("AT Strand" or ATS) are characterised by several main peaks representing different charge states of the strand (Section S6). When binding to each strand individually, complexes 1–6 were found to bind to up to one in every two base-pairs. For example, for the solutions of 9:1 PC to ATS strand ratio, the mass spectra for complex 2 produced peaks corresponding to as high as [ATS+9PC], while those for 5 only produced peaks for up to [ATS+7PC]. Spectra and relative abundance information can be found in Section S6.2. To determine if there was any base-pair preference, a competitive assay was carried out in which each PC was added to a 1:1 solution of the GCS and ATS strands. All of complexes 1–6 demonstrated the same behaviour in these experiments and so the spectra of complex 2 will be used as an example (Figure 12). Immediate observation of the mass spectra of 1:1 GCS to ATS with one and three equivalents of complex 2 suggests that there is GC selectivity; in the 1:1:1 spectrum the peaks

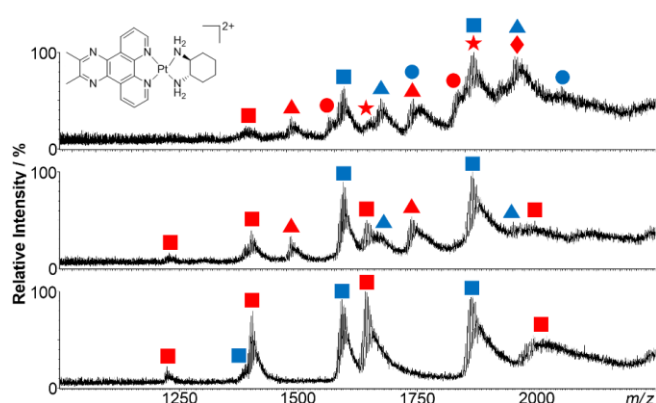


Figure 12. Mass spectra of a solution of complex 2, GCS (red symbols) and ATS (blue symbols) in the following ratios: 0:1:1 (bottom), 1:1:1 (middle) and 3:1:1 (top) (1 equivalent is 42 μ M). Legend: square = [DNA], triangle = [DNA+1PC], circle = [DNA+2PC], star = [DNA+3PC], diamond = [DNA+4PC].

corresponding to unbound GCS have dropped relative to the 0:1:1 spectrum while the ATS peaks are still at large. Supporting this, the peaks at 1482 and 1741 m/z in this spectrum correspond to [GCS+1PC]. There is evidence for [ATS+1PC] at ~ 1670 m/z , however this signal is also representative of unbound GCS and so the actual intensity would be quite low. The 3:1:1 spectrum further displays the GC selectivity of complex 2 as the ~ 1400 m/z peak representing unbound GCS at a charge of 7- has almost disappeared, while there is still some evidence of free ATS in the peaks at ~ 1660 and ~ 1800 m/z . Peaks corresponding to [ATS+1PC] (1666 and 1953 m/z) and [ATS+2PC] (1730 and 2050 m/z) are visible, however there are also peaks representative of [GCS+3PC] (1400 and 1870 m/z) and [GCS+4PC] (1950 m/z). GC selectivity is common for DNA intercalators,^[19] and these experiments were conducted within DNA:PC ratios in which only intercalation is occurring (in accordance with the LD experimental data). Abundances were not determined here as there are too many overlapping peaks; however it is clear that the PCs in this study selectively bind to GC base-pairs over AT ones.

In vitro cytotoxicity

As a continuation of the cytotoxicity assays performed in previous work with complexes 1–6 and 1'-6' in the L1210 murine leukaemia, HT29 human colon carcinoma and U87 human glioblastoma cell lines,^[5b] the activity of these complexes was assessed in a further ten cell lines: MCF-7 breast cancer, A2780 ovarian cancer, H460 lung cancer, A431 skin cancer, Du145 prostate cancer, BE2-C neuroblastoma, SJ-G2 human glioblastoma, MIA pancreas cancer, SMA murine glioblastoma and MCF10A breast (normal) (Table 3). These experiments were conducted to gain a greater understanding of the activity of 1–6 and 1'-6', to relate, if possible, the DNA affinity of 1–6 with their *in vitro* activity, and to determine particularly sensitive cell lines to target in further studies. For all cell lines studied, the complexes demonstrated potent, often sub-micromolar activity,

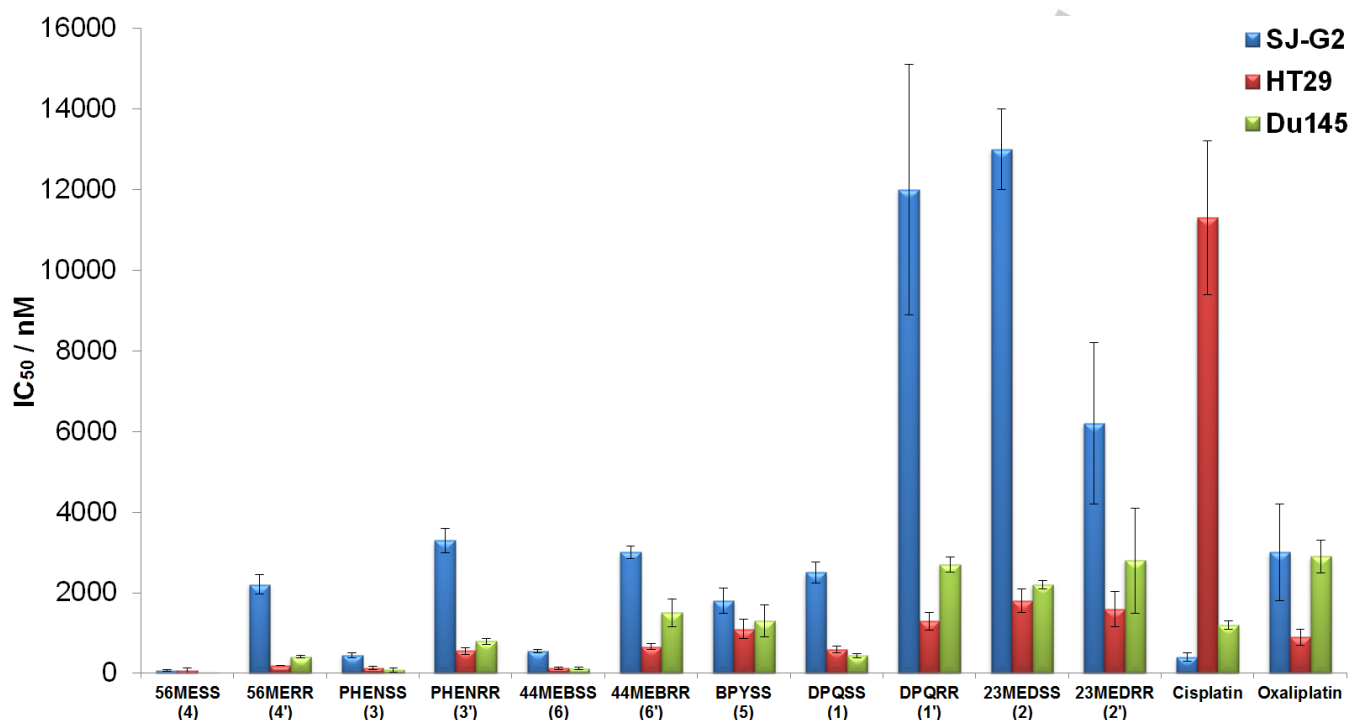


Figure 13. Comparison of the cytotoxicity of complexes 1–6 and 1'–6' in the SJ-G2 human glioblastoma (blue), HT29 colon carcinoma (red) and Du145 prostate cancer (green) cell lines, expressed as nanomolar IC_{50} values with standard error. Carboplatin and BPYRR (5) values have been omitted for clarity.

with complexes 3–6 demonstrating very high cytotoxicity in the Du145 prostate cancer (some values previously published^[20]), SJ-G2 glioblastoma, and the previously published HT29 colon carcinoma^[5b] lines (Figure 13). These cancer types are therefore good targets for further therapeutic studies. The lowest point of activity was in the BE2-C neuroblastoma line, with only complexes 3 and 4 reaching sub-micromolar IC_{50} concentrations. Also of note is the higher cytotoxicity of all PCs in the “normal” MCF10A breast cell line relative to the MCF-7 breast cancer line. This emphasises the importance of targeted delivery of these complexes to cancerous cells. Across the majority of cell lines, the same structure-activity trends are observed as previous studies: for P_{LS} , $56Me_2phen > phen \geq 44Me_2bpy > dpq > bpy \cong 23Me_2dpq$, and for A_{LS} , $SS-dach > RR-dach$. The fact that these trends were generally the same across all cell lines suggests that the *in vitro* mechanism of action of these PCs is largely independent of the cancer type, with minor differences between the mechanisms of individual complexes. A correlation between DNA affinity and cytotoxicity was observed for complexes 3–6; 4 and 5 were the most and least effective in both areas, respectively, while 3 and 6 were approximately equal in both DNA affinity and cytotoxicity. Interestingly, complexes 1 and 2 exhibited mid-low biological activity despite their relatively high DNA affinity. Additionally there were large differences in activity between *R,R* and *S,S* isomers, despite their similar DNA binding affinity as determined in our previous DNA study.^[6b] This reinforces the notion that the apoptotic mechanisms of these complexes involve much more than DNA binding alone.^[4, 21]

Further studies of the *in vitro* interactions of these complexes are warranted.

Conclusions

The DNA binding of six anticancer PCs DPQSS, 23MEDSS, PHENSS, 56MESS, BPYSS and 44MEBSS has been studied in depth through the use of several biophysical techniques. Overall, each technique contributed unique information regarding binding behaviour; LD, UV and ITC provided PC-DNA binding constant values, as well as binding mode and thermodynamic parameters. From this data it is clear that complexes 1–6 are capable of binding to DNA with an affinity of $\sim 10^5$ – 10^6 M^{-1} , with intercalation as the primary mode and other potential modes at higher PC concentrations. FID and SRCD experiments provided some insight into the effect of DNA affinity on the ability of the PCs to displace competing binders and to stabilise the DNA strand, respectively. Overall, 56MESS (4) and BPYSS (5) were found to be the most and least potent DNA binders, respectively. Finally, mass spectrometry studies revealed that each PC preferentially binds to GC base-pairs over AT ones. The unique information gleaned from each of these biophysical methods, and the minor differences in trends observed from each, clearly reveal that in order for one to have a complete understanding of the binding of small molecules to DNA, multiple techniques of analysis should be utilised. Complexes 1–6 and 1'–6' demonstrated high *in vitro*

Table 3. Summary of the *in vitro* cytotoxicity of complexes **1–6** and **1'–6'** in several cell lines, expressed as an IC₅₀ value with standard error (1 sig. fig.). IC₅₀ is the concentration at which cell growth is inhibited by 50% over 72 h.

Complex	IC ₅₀ (μM)												
	L1210 ^[a]	HT29 ^[a]	U87 ^[a]	MCF-7	A2780	H460	A431	Du145	BE2-C	SJ-G2	MIA	SMA	MCF10A
1 DPQSS	0.19 ± 0.01	0.59 ± 0.08	3.70 ± 0.24	1.8 ± 0.2	2.0 ± 0.1	1.9 ± 0.2	3.2 ± 0.2	0.44 ± 0.06	2.9 ± 0.2	2.5 ± 0.3	0.62 ± 0.03	1.3 ± 0.6	1.6 ± 0.2
1' DPQRR	0.8 ± 0.2	1.3 ± 0.2	12 ± 2.8	7.8 ± 0.8	6.5 ± 0.0	3.9 ± 0.2	7 ± 2	2.7 ± 0.2	24 ± 3	12 ± 3	2.3 ± 0.3	7 ± 2	6 ± 1
2 23MEDSS	1.3 ± 0.4	1.8 ± 0.3	8.2 ± 1.6	4.2 ± 0.4	3.7 ± 0.4	2.8 ± 0.1	13 ± 2	2.2 ± 0.1	34 ± 6	13 ± 1	0.7 ± 0.2	5.2 ± 0.4	4.3 ± 0.7
2' 23MEDRR	6 ± 2	1.6 ± 0.4	16 ± 3.2	4.4 ± 0.7	2.0 ± 0.1	8.0 ± 0.5	7 ± 2	3 ± 1	1.80 ± 0.06	6 ± 2	1.2 ± 0.3	2.1 ± 0.6	4 ± 1
3 PHENSS ^[b]	0.10 ± 0.01	0.13 ± 0.04	1.5 ± 0.4	0.5 ± 0.2	0.27 ± 0.03	0.5 ± 0.2	0.9 ± 0.3	0.08 ± 0.05	0.40 ± 0.05	0.45 ± 0.06	0.8 ± 0.7	0.24 ± 0.04	0.16 ± 0.07
3' PHENRR	1.5 ± 0.1	0.56 ± 0.08	8.9 ± 2.5	3.2 ± 0.2	2.70 ± 0.07	7.2 ± 0.9	2.0 ± 0.6	0.79 ± 0.08	3.8 ± 0.4	3.3 ± 0.3	2.7 ± 0.2	3.2 ± 0.3	2.4 ± 0.3
4 56MESS ^[b]	0.009 ± 0.002	0.08 ± 0.06	0.076 ± 0.014	0.05 ± 0.02	0.030 ± 0.004	0.037 ± 0.009	0.05 ± 0.02	0.007 ± 0.002	0.100 ± 0.002	0.07 ± 0.02	0.015 ± 0.002	0.032 ± 0.007	0.020 ± 0.005
4' 56MERR ^[b]	0.46 ± 0.01	0.19 ± 0.00	2.2 ± 0.058	0.8 ± 0.1	1.1 ± 0.1	1.8 ± 0.2	0.93 ± 0.03	0.41 ± 0.04	2.3 ± 0.2	2.2 ± 0.2	0.45 ± 0.006	1.6 ± 0.5	0.39 ± 0.01
5 BPYSS	0.6 ± 0.2	1.1 ± 0.2	4.0 ± 0.3	2.6 ± 0.2	2.6 ± 0.2	5 ± 2	3.1 ± 0.2	1.3 ± 0.4	3 ± 1	1.8 ± 0.3	2.5 ± 0.1	3.1 ± 0.8	1.6 ± 0.3
5' BPYRR ^[c]	5.5 ± 0.1	-	-	-	-	-	-	-	-	-	-	-	-
6 44MEBSS	0.36 ± 0.02	0.13 ± 0.03	0.500 ± 0.009	3.5 ± 0.7	0.9 ± 0.1	1.1 ± 0.3	0.5 ± 0.1	0.12 ± 0.03	1.0 ± 0.5	0.55 ± 0.04	3 ± 1	0.29 ± 0.03	0.27 ± 0.02
6' 44MEBRR	1.8 ± 0.0	0.66 ± 0.07	3.9 ± 0.4	2.70 ± 0.07	5 ± 1	5.6 ± 0.5	1.4 ± 0.4	1.5 ± 0.3	5.2 ± 0.4	3.0 ± 0.2	3.4 ± 0.2	2.7 ± 0.2	2.0 ± 0.3
Cisplatin	0.35 – 1 ^[d]	11 ± 2	3.8 ± 1.1	6.5 ± 0.8	1.0 ± 0.1	0.9 ± 0.2	2.4 ± 0.3	1.2 ± 0.1	1.9 ± 0.2	0.4 ± 0.1	8 ± 1	1.2 ± 0.1	nd
Oxaliplatin	nd	0.9 ± 0.2	1.8 ± 0.2	0.5 ± 0.1	0.16 ± 0.0	1.6 ± 0.1	4.1 ± 0.5	2.9 ± 0.4	0.9 ± 0.2	3 ± 1	0.9 ± 0.2	1.4 ± 0.1	nd
Carboplatin	nd	>50	>50	>50	9 ± 3	14 ± 1	24 ± 2	15 ± 1	19 ± 1	5.7 ± 0.2	>50	14.3 ± 0.7	nd

[a] – quoted from ref.^[6b] and those within.[b] – values for these complexes were also previously reported in ref.^[20]

[c] – pre-screening determined this complex was not active most Calvary Mater cell lines

[d] – values also retrieved from refs.^[6b, 22]

activity across a large range of human cancer cell lines with particularly high efficacy in Du145 prostate cancer and SJ-G2 glioblastoma cells. PCs of dpq and 23Me₂dpq, despite demonstrating relatively high DNA affinity, were among the least active biologically. For complexes of bpy, 44Me₂bpy, phen and 56Me₂phen, DNA affinity does appear to correlate with cytotoxicity, suggesting that DNA binding plays a role in the apoptotic activity of these complexes. However, the large difference in activity between enantiomers suggests that further studies of other, non-DNA interactions are needed to determine the overall mechanism of action.

Experimental Section

Materials and Preparation

All reagents were used as received and all solvents used were of analytical grade or higher. Complexes **1–6** and **1'–6'** were prepared as per previous publications.^[5b, 6b, 22] Dipotassium hydrogen orthophosphate, potassium dihydrogen orthophosphate, ammonium acetate, sodium fluoride, sodium chloride, D-10-camphorsulfonic acid, calf-thymus DNA and ethidium bromide (EtBr) were obtained from Sigma-Aldrich chemicals. Pora-Pak™ Rxn CX cartridges (20cc, 2g) were obtained from Waters. The HPLC-purified DNA oligonucleotides 5'-GCGCATGCGCATGCGC-3' ("GC Strand" or GCS) and 5'-GCATATGATATCATATGC-3' ("AT Strand or ATS") were obtained from Integrated DNA Technologies (IDT). Further purification and ion exchange of each strand was achieved by dissolution in 150 mM ammonium acetate and elution through a Pora-Pak™ Rxn CX cartridge (20cc, 2g) followed by lyophilisation. Annealing was achieved by heating solutions of each oligo in 150 mM ammonium acetate to 95 °C in a water bath for 3 min before leaving the water bath to cool overnight. Oligo concentrations were determined through UV absorbance, using the IDT-provided extinction coefficients of 254000 and 283000 M⁻¹cm⁻¹ per double strand at 260 nm for GCS and ATS, respectively. CT-DNA concentration was confirmed using the 260 nm extinction coefficient of 13200 M⁻¹cm⁻¹ per base pair.^[23] Ethidium bromide concentration was determined using the extinction coefficient of $\epsilon_{476} = 5680 \text{ M}^{-1}\text{cm}^{-1}$,^[24] and PC concentrations were determined using their respective extinction coefficients (Table 4).^[5b, 6b, 25]

Table 4. Wavelength maxima and extinction coefficients of complexes **1–6**.

No.	PL	$\lambda_{\text{max}} / \text{nm}$	$\epsilon / \text{M}^{-1} \text{cm}^{-1}$
1	Dpq	258	50000
2	23Me ₂ dpq	261	45000
3	Phen	226	35000
4	56Me ₂ phen	230	37000
5	Bpy	245	22000
6	44Me ₂ bpy	243	24500

Linear dichroism

LD spectra were obtained using a Jasco 810 spectropolarimeter using a quartz capillary LD Couette flow cell built by Crystal Precision Optics. Experiments at temperatures close to physiological resulted in DNA shearing, and so experiments were performed at 20 °C rather than 37 °C. The instrument was allowed to equilibrate for 30 min prior to use, and nitrogen gas flow was kept at $\sim 10 \text{ L min}^{-1}$. A series of ~ 17 solutions consisting of CT-DNA (150 μM), K₂HPO₄/KH₂PO₄ (10 mM, pH 7.3), NaCl (10 mM) and various amounts of each PC were prepared according to Table S1.1. NaCl concentration was relatively low due to the strong absorption of chloride salts at low wavelengths.^[26] For each solution, spectra were obtained over the range of 200–350 nm using a scan rate of 200 nm min⁻¹, data pitch of 1 nm, response time of 1 s and rotation speed of 3000 rpm. Two accumulations were collected and a baseline non-rotating spectrum was subtracted from each data set. The change of the DNA signal in proportion to the PC concentration was used to elucidate PC-DNA binding information, and to determine the binding constant for LD (K_{LD}). To determine the binding constants, the induced response of the LD signal was plotted against PC concentration, and fitted to the following equation using the published Wolfram *Mathematica* script,^[11] which utilises the binding model of Ismail and Stootman *et al.*^[11, 27]

$$\epsilon = 0.5R_B \left(\frac{1}{K} + \frac{B_T}{n} + L_T - \sqrt{\left(\frac{1}{K_{\text{LD}}} + \frac{B_T}{n} + L_T \right)^2 - \frac{4B_T L_T}{n}} \right)$$

where L_T is the total PC concentration, B_T is the total number of DNA bases, K_{LD} is the binding constant and n is the number of base-pairs per PC. R_B is the response of the instrument as a result of the binding of PC to DNA (whose concentration is denoted L_B) and ϵ is an experimental measurement that relates to L_B via:

$$\epsilon = R_B L_B$$

K_{LD} was calculated for each wavelength peak in the induced spectrum of complexes **1**, **3**, **5** and **6**. For all signals below 300 nm, the points of the binding curve corresponding to PC concentrations below 40 μM had to be removed in order to fit the data. The peak at $\sim 320 \text{ nm}$ for complexes **5** and **6** were not a result of DNA absorbance and so they could be fitted with all points below 40 μM . Experiments were performed in triplicate for each PC.

UV spectroscopy

Absorbance spectra were obtained using a Jasco V-660 UV/vis spectrometer operating at 37 °C. The wavelength range chosen was 200–450 nm, and the scan rate was 400 nm min⁻¹, data interval was 1 nm and averaging time was 0.1 s. The spectrum of each PC ($\sim 14 \mu\text{M}$) in K₂HPO₄/KH₂PO₄ (10 mM, pH 7.3) and NaCl (50 mM) buffer was initially obtained, followed by the titration of CT-DNA (1–2 mM) according to Table S2.1. The same amount of DNA and buffer was added to the reference cell to account for the absorbance of DNA. After each titration, the solutions were gently mixed and allowed to incubate for 2 min before measurement. The attenuation of signal at various wavelengths for each PC was used to determine the binding constant (K_{UV}) for each complex. The binding of each PC to CT-DNA was studied quantitatively using the same Wolfram *Mathematica* script as the LD experiments, to determine the binding constant (K_{UV}) and number of binding sites. It is important to note that many UV binding studies report much smaller changes in signal,

and so the script may not always be able to find a fit. Experiments were performed in triplicate for each PC.

Isothermal titration calorimetry assays

ITC traces were obtained using a MicroCal iTC 200 calorimeter operating at 37 °C. Each PC (600–750 μM) was titrated into a solution of CT-DNA (165 μM) in K₂HPO₄/KH₂PO₄ (10 mM, pH 7.3) and NaCl (50 mM) buffer. Each PC was also titrated into buffer without DNA for use as a baseline. The titration program consisted of one 0.4 μL addition followed by 18 titrations of 2 μL, with a spacing of 180 s, reference power of 6 μcal s⁻¹ and stirring speed of 750 rpm. Data was analysed using Origin 7.0 (MicroCal version) using 200 iterations of a one-site binding model using the following equations. Experiments were performed in duplicate for each PC.

$$\Delta G = -RT \ln K$$

$$\Delta S = \frac{\Delta H - \Delta G}{T}$$

Fluorescent intercalator displacement assays

Emission spectra for the FIDs were collected using a Jasco FP-2500 fluorimeter operating at 37 °C. The wavelength range chosen was 550–750 nm with an excitation wavelength of 480 nm, scan rate of 600 nm min⁻¹, data interval of 1 nm and averaging time of 0.1 s. The emission and excitation slits were each set to 5 nm. A solution of EtBr (75 μM) and CT-DNA (150 μM) in K₂HPO₄/KH₂PO₄ (10 mM, pH 7.3) and NaCl (50 mM) buffer was initially measured, followed by the titration of PC (various concentrations) according to Tables S4.1 and S4.2. After each titration the solution was gently mixed and incubated for 3 min before measurement. The attenuation of signal at 601 nm from each successive titration was used to calculate the binding constant for fluorescence (K_F). To determine the quenching mode, the Stern-Volmer equation was used:^[28]

$$\frac{F_0}{F} = 1 + K_q \tau_0 [PC] = 1 + K_{SV} [PC]$$

where F_0 is the fluorescence of the binding site in the absence of quencher, F is the fluorescence of the site containing the PC, K_q is the bimolecular quenching constant, τ_0 is the lifetime of the chromophore in the absence of the quencher ($\sim 22 \times 10^{-9}$ s for ethidium-bound DNA),^[29] and K_{SV} is the Stern-Volmer quenching constant. A plot of F_0/F against $[PC]$ using experimental values allows for the determination of K_q and K_{SV} from the slope. To determine K_F , the double-logarithm expression derived in our previous work was used to determine a binding constant for the PC-DNA interaction:^[6b]

$$\log_{10} \left(\frac{F_0 - F}{F} \right) = n \log_{10} [PC] + \log_{10} K_F$$

where n is the number of ethidium compounds displaced per PC. It is important to note that this expression is a simplification of the true binding interaction as the effect of EtBr on the binding equilibrium is ignored;^[30] however, the results obtained are still comparable between complexes of the same study.^[6b] A plot of $\log_{10}[(F_0 - F)/F]$ against

$\log_{10}[PC]$ is used to determine K_F and n from the intercept and slope, respectively. Experiments were performed in triplicate for each PC.

Synchrotron radiation circular dichroism

Experiments were performed at the AU-CD beamline on ASTRID2^[31] at ISA, Aarhus University. ASTRID2 operates in top-up mode with a current of 120 mA. The AU-CD beam line operates in the wavelength range of 125 to 450 nm, with a bandwidth of 0.6 nm. The beam size on the sample is 2 (vert.) × 6 (horz.) mm, with a sample to detector distance of 25 mm. All SRCD experiments were performed using a suprasil quartz cuvette with a 0.01 cm path length. Temperature control was achieved through the use of a Eurotherm temperature regulator. Calibration of the spectropolarimeter was assessed through daily measurement of the CD spectrum of D-10-camphorsulfonic acid. Each melting solution consisted of a PC (0.5 mM) and CT-DNA (1 mM) in K₂HPO₄/KH₂PO₄ (10 mM, pH 7.3) and NaF (50 mM) buffer. NaF was used due to the strong absorption of chloride salts at low wavelengths.^[26] Solutions of CT-DNA with no PC present were also measured. Temperature scans were performed as follows: the cell temperature began at 25 °C, was raised to 45 °C in 10 °C increments and then raised from 45–90 °C in 5 °C increments. The heating rate was 1 °C.min⁻¹. For each temperature increment, the cell was allowed to equilibrate for 5 min before a spectrum was recorded; these were collected from 350–170 nm with a 1 nm increment and three accumulations. Prior to each melting experiment, a baseline spectrum of the PC in phosphate buffer was obtained to partially eliminate the effects of PC chirality from the SRCD spectra. Experiments were performed in duplicate for each PC. For each wavelength, SRCD intensity was plotted against temperature, and a Boltzmann curve was fitted to the plot using Origin Pro 8.5 (Origin Labs) to determine the T_M . The CT-DNA concentration used here was much higher than that for other biophysical assays due to the lower path length of the cell used. To prevent the chirality of the PCs from affecting the CD spectrum of DNA, the PCs were included in the baseline solutions and the DNA:PC ratio was consistently kept at 2:1 and no higher.

Electrospray Ionisation Mass Spectrometry

DNA-PC solutions were analysed *via* negative-mode ESIMS using a Waters XEVO QToF ESI mass spectrometer with a Z-spray ionisation source. Mass spectra were obtained with a MCP potential of 2400 V, a cone voltage of 25 V and a capillary tip potential of 2.4 kV. The desolvation gas flow was 300 L/h at a desolvation temperature of 150 °C with the source temperature at 70 °C. The collision energy was set to off. Spectra were obtained over a mass/charge (m/z) range of 50–4000. A Hamilton 250 μL model 1725RN gastight syringe was loaded with 25 μL of solution and infused into the mass spectrometer source using a KD Scientific model 100 syringe pump set to 5 μL min⁻¹, achieving 5 minutes of data acquisition. Between each run the syringe was cleaned thoroughly and the mass spectrometer was flushed with MilliQ-purified water.

In-vitro cytotoxicity

Cytotoxicity assays were performed at the Calvary Mater Newcastle Hospital, Waratah, NSW, Australia. The cell lines tested were MCF-7 breast cancer, A2780 ovarian cancer, H460 lung cancer, A431 skin cancer, Du145 prostate cancer, BE2-C neuroblastoma, SJ-G2 glioblastoma, MIA pancreas cancer, SMA murine glioblastoma and the non-tumour derived MCF10A breast cell lines. All test agents were prepared as 30 mM stock solutions in DMSO and stored at -20 °C. Cell lines were cultured in a humidified atmosphere 5% CO₂ at 37 °C and maintained in Dulbecco's modified Eagle's medium (Trace Biosciences,

Australia) supplemented with 10% foetal bovine serum, 10 mM sodium bicarbonate penicillin (100 IU mL⁻¹), streptomycin (100 µg mL⁻¹), and glutamine (4 mM). Cytotoxicity was determined by plating cells in duplicate in 100 mL medium at a density of 2,500–4,000 cells per well in 96 well plates. On day 0, (24 h after plating) when the cells were in logarithmic growth, 100 µL medium with or without the test agent was added to each well. After 72 h drug exposure growth inhibitory effects were evaluated using the MTT (3-[4,5-dimethylthiazol-2-yl]-2,5-diphenyl-tetrazolium bromide) assay and absorbance read at 540 nm. An eight point dose response curve was produced from which the IC₅₀ value was calculated, representing the drug concentration at which cell growth was inhibited by 50% based on the difference between the optical density values on day 0 and those at the end of drug exposure.^[32]

Acknowledgements

The authors thank ISA, Aarhus University for synchrotron beam time and Australian Synchrotron for providing International Synchrotron Access project travel funds. We also thank Western Sydney University for its financial support through internal research grants. B.J.P. and D.L.A. were supported by an Australian Postgraduate Award and Western Sydney University Top-Up Award. B.J.P. was also supported by an Endeavour Fellowship.

Keywords: DNA • anticancer • spectroscopy • biophysical • platinum

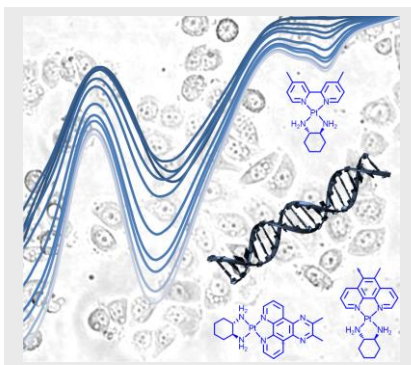
- [1] a) B. H. Harper, F. Li, R. Beard, K. B. Garbutcheon-Singh, N. S. Ng, J. R. Aldrich-Wright in *Biomolecular Interactions of Platinum Complexes*, (Ed. H. J. Schneider), Royal Society of Chemistry, Cambridge, UK, **2013**; b) A. Callejo, L. Sedó-Cabezón, I. D. Juan, J. Llorens, *Toxics* **2015**, *3*, 268-293.
- [2] a) A. M. Krause-Heuer, R. Grünert, S. Kühne, M. Buczkowska, N. J. Wheate, D. D. Le Pevelen, L. R. Boag, D. M. Fisher, J. Kasparkova, J. Malina, P. J. Bednarski, V. Brabec, J. R. Aldrich-Wright, *J. Med. Chem.* **2009**, *52*, 5474-5484.; b) L. A. Graham, J. Suryadi, T. K. West, G. L. Kucera, U. Bierbach, *J. Med. Chem.* **2012**, *55*, 7817-7827.
- [3] C. R. Brodie, J. G. Collins, J. R. Aldrich-Wright, *Dalton Trans.* **2004**, 1145-1152.
- [4] K. B. Garbutcheon-Singh, S. Myers, B. W. J. Harper, N. S. Ng, Q. Dong, C. Xie, J. R. Aldrich-Wright, *Metallomics* **2013**, *5*, 1061-1067.
- [5] a) K. B. Garbutcheon-Singh, B. W. J. Harper, S. Myers, J. R. Aldrich-Wright, *Metallomics* **2014**, *6*, 126-131.; b) B. J. Pages, Y. Zhang, F. Li, J. Sakoff, J. Gilbert, J. R. Aldrich-Wright, *Eur. J. Inorg. Chem.* **2015**, *2015*, 4167-4175.
- [6] a) S. Kemp, N. J. Wheate, D. P. Buck, M. Nikac, J. G. Collins, J. R. Aldrich-Wright, *J. Inorg. Biochem.* **2007**, *101*, 1049-1058.; b) B. J. Pages, F. Li, P. Wormell, D. L. Ang, J. K. Clegg, C. J. Kepert, L. K. Spare, S. Danchaiwijit, J. R. Aldrich-Wright, *Dalton Trans.* **2014**, *43*, 15566-15575.
- [7] a) D. Z. M. Coggan, I. S. Haworth, P. J. Bates, A. Robinson, A. Rodger, *Inorg. Chem.* **1999**, *38*, 4486-4497.; b) S. M. Kelly, T. J. Jess, N. C. Price, *Biochim. Biophys. Acta, Proteins Proteomics* **2005**, *1751*, 119-139.; c) N. Shahabadi, L. Heidari, *Spectrochim. Acta A* **2014**, *128*, 377-385.
- [8] B. J. Pages, D. L. Ang, E. P. Wright, J. R. Aldrich-Wright, *Dalton Trans.* **2015**, *44*, 3505-3526.
- [9] B. Norden, A. Rodger, T. Dafforn, *Linear dichroism and circular dichroism – A textbook on polarised-light spectroscopy*, The Royal Society of Chemistry, London, **2010**, p. 304.
- [10] a) T. Biver, *Appl. Spectrosc. Rev.* **2012**, *47*, 272-325.; b) M. R. Gill, D. Cecchin, M. G. Walker, R. S. Mulla, G. Battaglia, C. Smythe, J. A. Thomas, *Chem. Sci.* **2013**, *4*, 4512-4519.
- [11] D. L. Ang, N. C. Jones, F. Stootman, B. Ghadirian, J. R. Aldrich-Wright, *Analyst* **2015**, *140*, 4162-4169.
- [12] N. C. Garbett, J. B. Chaires, *Expert Opin. Drug Discovery* **2012**, *7*, 299-314.
- [13] J. A. D'Aquino, E. Freire, L. M. Amzel, *Proteins* **2000**, *Suppl. 4*, 93-107.
- [14] R. W. Sabnis, *Handbook of Biological Dyes and Stains: Synthesis and Industrial Applications*, John Wiley & Sons, New Jersey, **2010**, p. 544.
- [15] a) J. B. Lepecq, C. Paoletti, *J. Mol. Biol.* **1967**, *27*, 87-106.; b) R. R. Monaco, *J. Biomol. Struct. Dyn.* **2007**, *25*, 119-125.
- [16] W. R. Ware, *J. Phys. Chem.* **1962**, *66*, 455-458.
- [17] D. L. Ang, B. W. J. Harper, L. Cubo, O. Mendoza, R. Vilar, J. Aldrich-Wright, *Chem. Eur. J.* **2015**, 2317-2325.
- [18] a) S. M. Meier, M. Hanif, Z. Adhireskan, V. Pichler, M. Novak, E. Jirkovsky, M. A. Jakupec, V. B. Arion, C. A. Davey, B. K. Keppler, C. G. Hartinger, *Chem. Sci.* **2013**, *4*, 1837-1846.; b) K. J. Davis, C. Richardson, J. L. Beck, B. M. Knowles, A. Guedin, J.-L. Mergny, A. C. Willis, S. F. Ralph, *Dalton Trans.* **2015**, *44*, 3136-3150.
- [19] a) K. X. Chen, N. Gresh, B. Pullman, *FEBS Lett.* **1987**, *224*, 361-364.; b) R. Nanjunda, W. D. Wilson in *Binding to the DNA Minor Groove by Heterocyclic Dications: From AT Specific Monomers to GC Recognition with Dimers*, John Wiley & Sons, Inc., New York, USA, **2012**.
- [20] F. J. Macias, K. M. Deo, B. J. Pages, P. Wormell, J. K. Clegg, Y. Zhang, F. Li, G. Zheng, J. Sakoff, J. Gilbert, J. R. Aldrich-Wright, *Chem. Eur. J.* **2015**, *21*, 16990-17001.
- [21] a) S. Wang, M. J. Wu, V. J. Higgins, J. R. Aldrich-Wright, *Metallomics* **2012**, *4*, 950-959.; b) K. J. Davis, J. A. Carrall, B. Lai, J. R. Aldrich-Wright, S. F. Ralph, C. T. Dillon, *Dalton Trans.* **2012**, *41*, 9417-9426.
- [22] N. J. Wheate, R. I. Taleb, A. M. Krause-Heuer, R. L. Cook, S. Wang, V. J. Higgins, J. R. Aldrich-Wright, *Dalton Trans.* **2007**, 5055-5064.
- [23] T. Maniatis, E. F. Fritsch, J. Sambrook, *Molecular Cloning: A Laboratory Manual*, Cold Spring Harbor Laboratory, NY, USA, **1982**, p. 545.
- [24] C. Y. Lee, H.-W. Ryu, T.-S. Ko, *Bull. Korean Chem. Soc.* **2001**, *22*, 87-89.
- [25] K. B. Garbutcheon-Singh, P. Leverett, S. Myers, J. R. Aldrich-Wright, *Dalton Trans.* **2013**, *42*, 918-926.
- [26] S. M. Kelly, N. C. Price, *Curr. Protein Pept. Sci.* **2000**, *1*, 349-384.
- [27] a) M. A. Ismail, K. J. Sanders, G. C. Fennell, H. C. Latham, P. Wormell, A. Rodger, *Biopolymers* **1998**, *46*, 127-143.; b) F. H. Stootman, D. M. Fisher, A. Rodger, J. R. Aldrich-Wright, *Analyst* **2006**, *131*, 1145-1151.
- [28] O. Stern, M. Volmer, *Phys. Z.* **1919**, *20*, 183-188.
- [29] D. P. Heller, C. L. Greenstock, *Biophys. Chem.* **1994**, *50*, 305-312.
- [30] a) W. C. Tse, D. L. Boger, *Acc. Chem. Res.* **2003**, *37*, 61-69.; b) B. K. S. Yeung, W. C. Tse, D. L. Boger, *Bioorg. Med. Chem. Letters* **2003**, *13*, 3801-3804.; c) S. P. Sau, P. Kumar, P. K. Sharma, P. J. Hrdlicka, *Nucleic Acids Res.* **2012**, *40*, e162.
- [31] a) A. J. Miles, S. V. Hoffmann, Y. Tao, R. W. Janes, B. A. Wallace, *Spectrosc.* **2007**, *21*, 245-255.; b) A. J. Miles, R. W. Janes, A. Brown, D. T. Clarke, J. C. Sutherland, Y. Tao, B. A. Wallace, S. V. Hoffmann, *J. Synchrotron Radiat.* **2008**, *15*, 420-422.
- [32] M. Tarleton, J. Gilbert, M. J. Robertson, A. McCluskey, J. A. Sakoff, *MedChemComm* **2011**, *2*, 31-37.

Entry for the Table of Contents (Please choose one layout)

Layout 1:

FULL PAPER

DNA binding behaviour of six polyaromatic platinum anticancer complexes has been studied using six biophysical methods (linear dichroism pictured), resulting in a comparison of the merits of each technique and the establishment of trends in DNA affinity in relation to complex structure. *In vitro* cytotoxicity in a panel of human cells was determined, revealing sub-micromolar activity in Du145 and SJ-G2 cells. Correlations between activity and DNA affinity were determined.



Benjamin J. Pages, Jennette Sakoff, Jayne Gilbert, Alison Rodger, Nikola P. Chmel, Nykola C. Jones, Sharon M. Kelly, Dale L. Ang, Janice R. Aldrich-Wright.*

Page No. – Page No.

Multifaceted studies of the DNA interactions and *in vitro* cytotoxicity of anticancer polyaromatic platinum(II) complexes